CHITOSAN/HYDROXYAPATITE COMPOSITE GRAFTS FOR BONE TISSUE ENGINEERING

Alina Florentina VLADU[1,4], Ludmila MOTELICA[2,4,5], Ovidiu-Cristian OPREA[2,4,5,6], Roxana Doina TRUŞCĂ[1,2], Florin IORDACHE[7,8], Denisa FICAI [2,4,5,6], Anton FICAI [1,2,4,5*]

This study's aim was to develop some chitosan/hydroxyapatite (CS/HAp) based composite systems for bone tissue regeneration by freeze drying method following the in situ synthesis of hydroxyapatite. The structures were morphologically and structurally characterized by Fourier transform infrared spectroscopy (FTIR), thermogravimetric analysis (TGA) scanning electron microscopy (SEM), and biologically by determining their biocompatibility through XTT and LDH assays. The FTIR spectra revealed the characteristic peaks of HAp at 553, 614 cm^{-1}, 1018 cm^{-1}, 1548 and 1410 cm^{-1}. SEM images illustrate the open structure, with interconnected pores and good pores distribution. The inorganic phase contains spheres and rods in the nanometric range. Samples showed very good biocompatibility with over 90% viability and low cytotoxicity in the case of composite systems.

Keywords: composite materials, bone tissue engineering, chitosan, *in situ* hydroxyapatite synthesis

1. Introduction

Over the last several decades, there have been an increasing number of people, millions worldwide, who have been affected by bone-related conditions,

* Corresponding author
[1] Science and Engineering of Oxide Materials and Nanomaterials, Faculty of Chemical Engineering and Biotechnologies, National University of Science and Technology POLITEHNICA Bucharest, Romania, alina_vladu_1995@yahoo.com, motelica_ludmila@yahoo.com, truscaroxana@yahoo.com, antonficai@upb.ro
[2] National Center for Micro and Nanomaterials, National University of Science and Technology POLITEHNICA Bucharest, Romania
[3] The National Research and Development Institute for Textiles and Leather, Bucharest, Romania
[4] National Center for Scientific Research for Food Safety, National University of Science and Technology POLITEHNICA Bucharest, Romania
[5] Academy of Romanian Scientists, Bucharest, Romania
[6] Department of Inorganic Chemistry, Physical Chemistry and Electrochemistry, Faculty of Chemical Engineering and Biotechnologies, National University of Science and Technology POLITEHNICA Bucharest, Romania, ovidiu73@yahoo.com denisaficai@yahoo.ro
[7] Biochemistry Disciplines, Faculty of Veterinary Medicine, University of Agronomic Sciences and Veterinary Medicine, Bucharest, Romania, floriniordache84@yahoo.com
[8] Advanced Research Center for Innovative Materials, Products and Processes CAMPUS, National University of Science and Technology POLITEHNICA University, Bucharest, Romania

most of them being caused by trauma, infections, accidents, degenerative diseases and cancers. Each year, approximately 2.2 million orthopedic medical procedures are done, with at least 500,000 bone grafting interventions taking place in the USA alone [1]. Conventional approaches, such as the use of autografts and allografts, are still considered the gold standard in orthopedics, but have a series of disadvantages, such as limited availability, immune response, donor site morbidity, disease transmission, foreign body rejection and infection risks [2]. In the continuously evolving field of biomedical research, a special interest was given to the regeneration of affected bone tissue and innovative treatments are actively pursued. From various approaches, bone tissue engineering (BTE) stands out as a promising solution. This type of treatment uses biomaterial-based strategies, which have allowed the development of suitable constructs that facilitate cell adhesion, cell proliferation, and differentiation [3].To overcome the potential issues, several synthetic materials, especially bioceramics, have been proposed, being available in different forms such as scaffolds, spheres, cement and bulk materials [4, 5, 6]. Moreover, these biomaterials are able to facilitate the sustained release of certain proteins such as growth factors, which are very important for supporting effective bone tissue regeneration and healing [7]. Natural bone tissue is made up an inorganic phase, respectively calcium-deficient carbonated hydroxyapatite and a main organic component, which is type I collagen. The main goal of developing scaffolds for bone tissue engineering is to reproduce these complex features through a biomimetic approach. Calcium phosphates are used on a large scale to replicate the inorganic phase of natural bone, while both synthetic and natural biodegradable polymers are aimed to mimic the organic phase. Among these, natural polymers such as collagen, alginate, chitosan, and gelatin, have gained a growing interest due to their great biocompatibility and ability to create effective composites together with calcium phosphates. Chitosan, a natural polymer has been extensively studied and involved in the development of biomimetic scaffolds for BTE. Due to its remarkable properties, chitosan was used for developing many kinds of biomaterials, such as molded macroporous structures, microspheres, hydrogels, fibrous forms and 3D-printed scaffolds, each addressing particular regenerative applications [8]. Chitosan is a natural polymer, a polysaccharide, derivative of chitin and is frequently obtained by extraction from the cell walls of fungi and the shells of crustaceans. Regarding its structure, chitosan is made of units of β-(1-4)-linked D-glucosamine and N-acetyl-d-glucosamine. Therefore, its structure is almost identical to glycosaminoglycan, an essential component of the cell surface and bone matrix. This resemblance to glycosaminoglycans makes chitosan efficient in regulating the activity of various osteoclastic and osteogenic factors, confirming its choice as a material in bone tissue engineering [9, 10]. The linear structure of pure chitosan has reduced mechanical strength, making it less

effective for BTE applications [11]. To improve the mechanical characteristics of chitosan, chemical crosslinkers such as genipin, dextrins and purines can be used. They help to connect the devided chains of chitosan, increasing its mechanical characteristics. When combined with different additives, these crosslinkers improve the strength of chitosan scaffolds, while maintaining their biocompatibility, moldability, biodegradability and antibacterial properties [12].

Human bones contain around 70% inorganic components, mainly doped hydroxyapatite (HAp), and ~21% organic components, including collagen fibers and bone marrow cells and 9%water. Studies have shown that HAp is superior to other widely used biomaterials like polylactic acid, hydrogels, and nanofiber composites in terms of reparative capacity of bones and cartilage [13, 14]. HAp is a natural inorganic calcium phosphate and a key constituent of human bone due to its biocompatibility and bioactivity [15, 16, 17]. Considering that the bone is composed of organic and inorganic components, composite materials such as chitosan and hydroxyapatite are well-suited to be used as orthopedic surgical implants [18]. Szatkowski et al. fabricated some composites by incorporating HAp plates with dimensions of 500 nm to 5 μm inside the chitosan matrix. They used a one-step co-precipitation technique involving disodium hydrogen phosphate and calcium chloride. The results revealed that this biomaterial is suitable for biomedical applications [19]. Hu et al. synthesized a hybrid scaffold, which mimics the bone structure containing chitosan, nano-hydroxyapatite (nHAp), hyaluronic acid and chondroitin sulfate by freeze-drying technique. This scaffold showed improved osteoblast proliferation, differentiation, and great mechanical properties. The study demonstrated the important role of pore size and porosity in maximizing nutrient transport within bone scaffolds. Moreover, the distribution of nanosized particles inside the scaffold was uniform and there was no agglomeration in the homogeneously interconnected microstructure [20]. El-Meliegy et al. [20] studied the enhancement of physico-chemical characteristics of some freeze-dried composite scaffolds made of chitosan and dextran through the incorporation of nano-hydroxyapatite. The results emphasized that the nanocomposites possess desirable porosity which allows the proliferation of bone cells and nutrient passage and increased compressive strength. Abdian et al. [21] reported that scaffolds comprised of mesoporous silica and hydroxyapatite nanoparticles obtained by freeze drying technique exhibited suitable cells adhesion, distribution and proliferation. *In vivo* results revealed great bone regeneration potential. Du et al. used a water/oil emulsion technique to develop composite spheres based on carbonated hydroxyapatite and chitosan, with diameters between 100–200 μm and 300–400 μm, used as fillers for bone regeneration. Although the diameter of the spheres did not impair their biodegradation, the pH of the buffer significantly affected the degradation rate [22, 23]. Wang et al. obtained a composite scaffold made of HAp and CS with a

3D porous structure. They used no chemical crosslinkers and the HAp microspheres, characterized by an increased surface area and urchin-like microstructure, were primarily synthesized via a hydrothermal method. The microspheres were subsequently incorporated into the CS matrix to obtain the HAp/CS composite scaffolds by a freeze-drying technique, leading to scaffolds with large pore sizes, interconnected pores, and increased porosity. At a 3% HAp content, the compressive elastic modulus of the scaffold increased. The incorporation of HAp microspheres enhanced cell adhesion and promoted the formation of osteoblasts. Besides, periostin could be incorporated onto the scaffolds, improving its controlled release during bone regeneration. *In vivo* analysis revealed that the loading of periostin in HAp/CS scaffolds reduced bone resorption, facilitated the proliferation of osteoblasts, induced osteointegration, and enhanced bone regeneration [24].

The present study focuses on developing composite materials for hard tissue engineering starting from chitosan and the *in situ* synthesized hydroxyapatite with the final aim to extend these studies by loading these composites with a mixture of natural/synthetic active compounds and used in the treatment of different diseases specific for bones.

2. Materials and methods

2.1. Materials

The synthesis of chitosan/hydroxyapatite (CS/HAp) based composite systems was achieved using chitosan of medium molecular weight, 75-85% deacetylated from Sigma-Aldrich, calcium hydroxide - $Ca(OH)_2$ of ≥ 96% purity from Fluka, di-ammonium hydrogen phosphate - $(NH_4)_2HPO_4$ of ≥ 97% purity from Roth. Acetic acid glacial – CH_3COOH ≥ 99% reagent grade and ammonium hydroxide solution – NH_4OH ~ 25% NH_3 basis were purchased from Sigma-Aldrich.

2.2. Methods

Chitosan/hydroxyapatite based composite systems of different ratios (1:3 and 3:1) were synthesized by freeze drying technique, the workflow being presented in Fig 1. First, 2 wt.% chitosan solution was dissolved in 1% (v/v) glacial acetic acid by stirring for 24 h. For the *in situ* synthesis of hydroxyapatite, calcium hydroxide – $Ca(OH)_2$ was suspended in distilled water while the pH was maintained slightly acid and then added dropwise in the chitosan solution and stirred for 1 h. Also, the phosphate solution was obtained by dissolving the required amount of $(NH_4)_2HPO_4$ in distilled water and ammonium hydroxide. After obtaining the chitosan-Ca^{2+} solution the gel was poured in a 45 mm Büchner funnel who`s bottom was covered with filter paper and immersed in a 200 mL beaker containing the $(NH_4)_2HPO_4$ solution. This process allows the diffusion of

phosphate solution inside the gel through the Büchner`s holes. After the chitosan precipitation and formation of the solid gel containing the calcium phosphate, it was freeze dried using a Martin Christ Alpha 2-4 LSC lyophilizer. The obtained composite structures were further characterized by FT-IR, thermogravimetric analysis, SEM and regarding their biocompatibility by XTT and LDH assays.

Fourier Transformed Infrared Spectroscopy (FT-IR)

FT-IR was used to determine the existence of specific functional chemical groups in the prepared samples. For this purpose, a Nicolet iS50 FTIR spectrometer was used. This device is fitted with a DTGS detector, offering high sensitivity across the 4000 cm^{-1} to 400 cm^{-1} range with a 4 cm^{-1} resolution. To enhance spectral quality, 32 scans were summed. Measurements were conducted at room temperature, with data recording and analysis carried out using Omnic32 software.

Thermogravimetric analysis

For this analysis, around 10 mg of each specimen was introduced in an open alumina crucible contained by a Netzsch STA 449C Jupiter apparatus (Selb, Germany). The specimens were heated starting from room temperature to 900°C with a temperature increase of 10 $K \cdot min^{-1}$ under a continuous flow of 50 $mL \cdot min^{-1}$ dried air. In addition, an empty alumina crucible served as the reference.

Scanning electron microscopy (SEM)

The obtained samples were characterized by SEM to illustrate the surface morphology of the obtained composite structures, the distribution of hydroxyapatite in the polymer matrix, and the evaluation of the appearance and size of the pores. Images were captured by a Quanta Inspect F50 scanning electron microscope, which is fitted with a field emission gun offering 1.2 nm resolution. The energy dispersive X-ray spectrometer provided with the equipment has a MnK resolution of 133 eV.

Biocompatibility evaluation

Cell viability and proliferation XTT assay and lactate dehydrogenase (LDH) cytotoxicity assay were performed to determine the biocompatibility of the tested samples. CyQUANT™ XTT Cell Viability Assay kit and CyQUANT™ LDH Cytotoxicity Assay Kit were used, and an osteoblast cell line was selected for this purpose. Cell viability was assessed after 48 h by measuring absorbance at 450 nm. Cytotoxicity was assessed after 24 h, using a microplate reader, by measuring the absorbance of 490 nm and 680 nm.

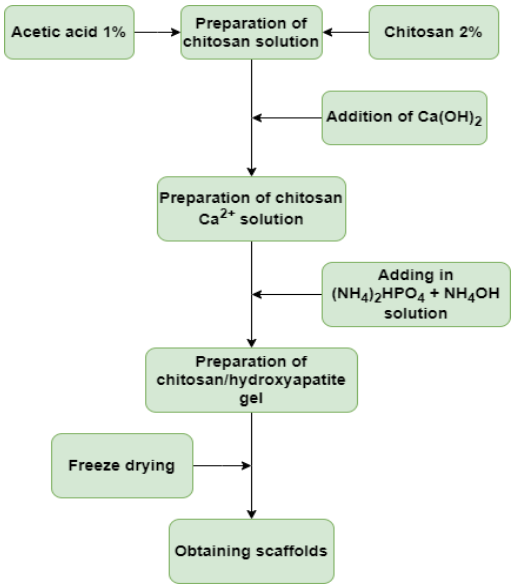

Fig. 1. Synthesis of CS/HAp composite materials

3. Results and discussion

The obtained composite systems were structurally, morphologically and biologically analyzed to determine their potential use as bone substitutes. FT-IR analysis gave information about the presence of chitosan and hydroxyapatite characteristic bands.

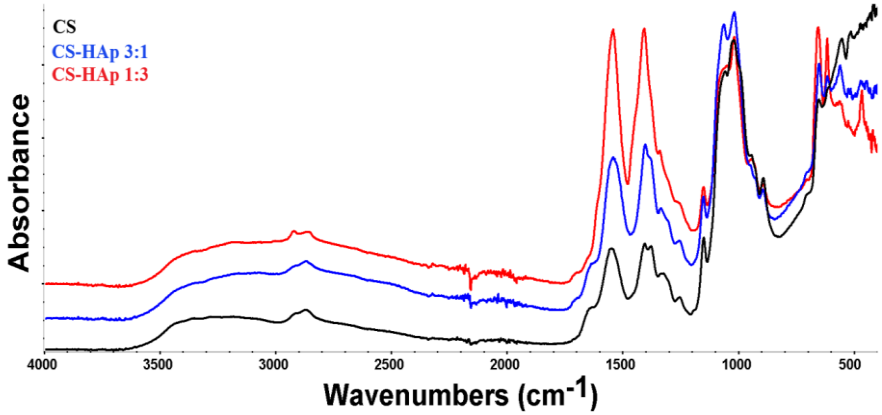

Fig. 2. FTIR spectra of CS (black), CS/HAp 1:3 (red) and CS/HAp 3:1 bleu)

Analyzing the FT-IR spectra (Fig. 2) acquired for the composite structures the specific bands for the organic and inorganic phases can be observed. The broad band found in the 3125–3325 cm^{-1} region is indicative for the stretching of N-H and O-H bonds, along with chitosan's specific intramolecular hydrogen bonds. The absorption peaks indicated at 2864, and 2922 cm^{-1} are associated with

C-H asymmetric and symmetric stretching. There are two strong adsorption bands at 1541 and 1402 cm^{-1}. The sharp maximum observed at 1541 cm^{-1} can be assigned to amide II or N-H bending, possibly linked to $-NH_3^+$ cation deformation in CS (protonated amino groups), while the adjacent maximum from 1402 cm^{-1} corresponds to C-H bending or carboxylic acid (HCOO−) bonds. There is also an overlap of certain characteristic bands, common to both the organic and inorganic groups: carbonate–chitosan ν_3 (CO_3^{2-}) in the range 1400–1580 cm^{-1} and 1350–1550 cm^{-1}). A tiny shoulder found at 1643 cm^{-1} resulted from amide I or C=O vibrations, while the small absorption band at 1151 cm^{-1} was due to the stretching of C-O bond. At the same time, hydroxyapatite's presence can be determined by the bands at 655, 615 and 560 cm^{-1} (ν_4 (PO_4^{3-})), 960 cm^{-1} corresponding to the brushite (HPO_4^{2-}), 1018 cm^{-1} (ν_3 (PO_4^{3-})). The band at 875 cm^{-1} could belong to HPO_4^{2-} species, showing the nonstoichiometric nature of the HA specimen, but can also be assigned to carbonate group (ν_2 (CO_3^{2-})).

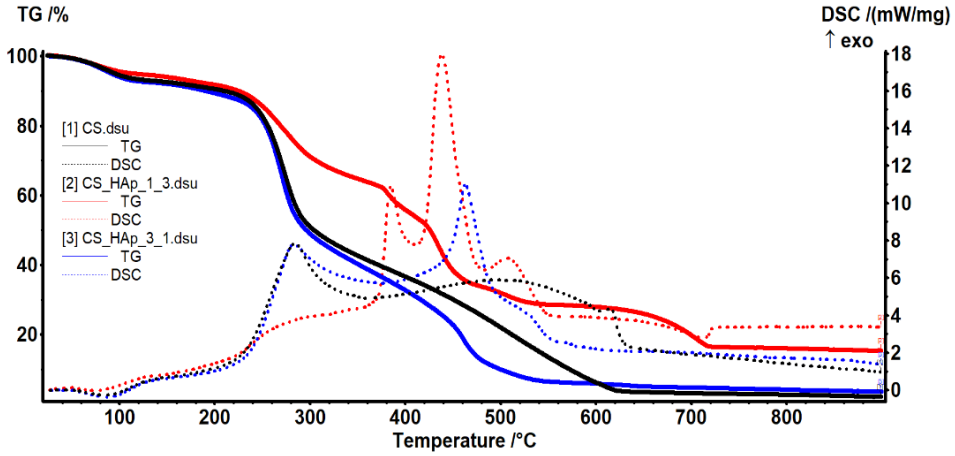

Fig. 3. The TG-DSC curves for the composite systems based on CS and HAp

The main numerical data acquired from thermal analysis are shown in Table 1.

Table 1

Residual mass and estimated load (% HAp)

Sample	Mass loss (%) RT-220°C	Endo (°C)	Mass loss (%) 220-360°C	Exo I (°C)	Mass loss (%) 360-630°C	Exo II (°C)	Residual mass (%)	Estimated load (% HAp)
CS	10.75	84.8	47.86	284.2	37.84	499.0	2.02	-
CS/HAp 3:1	12.19	87.0	49.03	282.8	33.45	463.2	3.56	1.67
CS/HAp 1:3	9.56	75.0	26.65	283.0	36.84	438.3	15.29	14.43

As it can be observed from Fig. 3, the chitosan sample is losing water up to 220°C, which is emphasized by the endothermic phenomenon from 84.8°C.

After 220°C the sample oxidative degradation begins. Between 220-360°C a mass loss of 47.86% is recorded due to the polymer backbone fragmentation, accompanied by the oxidation of the less stable fragments. In this process a strong exothermic response with the maximum at 284.2°C is observable on the DSC curve, indicating the dominance of the oxidation reactions. Between 360-630°C a steady mass loss is recorded, amounting 37.84% of the initial mass. The process exhibits a broad and intense exothermic effect on the DSC curve, with a maximum at 499°C. This process can be assigned to the oxidation of the residual carbonaceous mass [25].

The thermal analysis for the CS/HAp 3:1 sample is rather similar with that of CS due to the low HAp content. Therefore, up to 220°C a mass loss of 12.19% is observed, which has an associated endothermic effect at 87.0°C. This process is assigned to the loss of water trapped into the chitosan matrix. Between 220-360°C the main mass loss step occurs, amounting to 49.03% from the initial mass. The exothermic effect from 282.8°C indicates that the oxidative reactions occur in this step. Between 360-630°C a mass loss of 33.45% is recorded, the corresponding exothermic effect from 463.2°C suggesting the oxidation of the carbonaceous residual mass. The estimation of the HAp content is 1.67%.

The higher HAp containing sample, CS/HAp 1:3, presents a different behaviour at higher temperatures. Up to 220°C a dehydration process occurs, the registered mass loss being 9.56%, with an endothermic effect at 75°C. The polymer backbone fragmentation and oxidation process between 220-360°C takes place slower and with a lower recorded mass loss, of 26.65%. Due to the lower intensity, the exothermic effect of this process is observable as a shoulder at 283°C. After 360°C a more complex degradation step occurs, accompanied by three exothermic effects at 385.1, 438.3 and 506.8°C, indicating the presence of at least three separate reactions, due to the interactions of CS and subsequent fragments with HAp. The recorded mass loss is 36.84%. The interaction of CS with HAp can be also deduced from the last decomposition step between 630-900°C, which was not present in the other samples. A mass loss of 11.67% is observed in this interval, accompanied by an endothermic effect at 712.4°C, indicating a possible decomposition of carbonates from the HAp surface. The estimation of the HAp content is 14.43%.

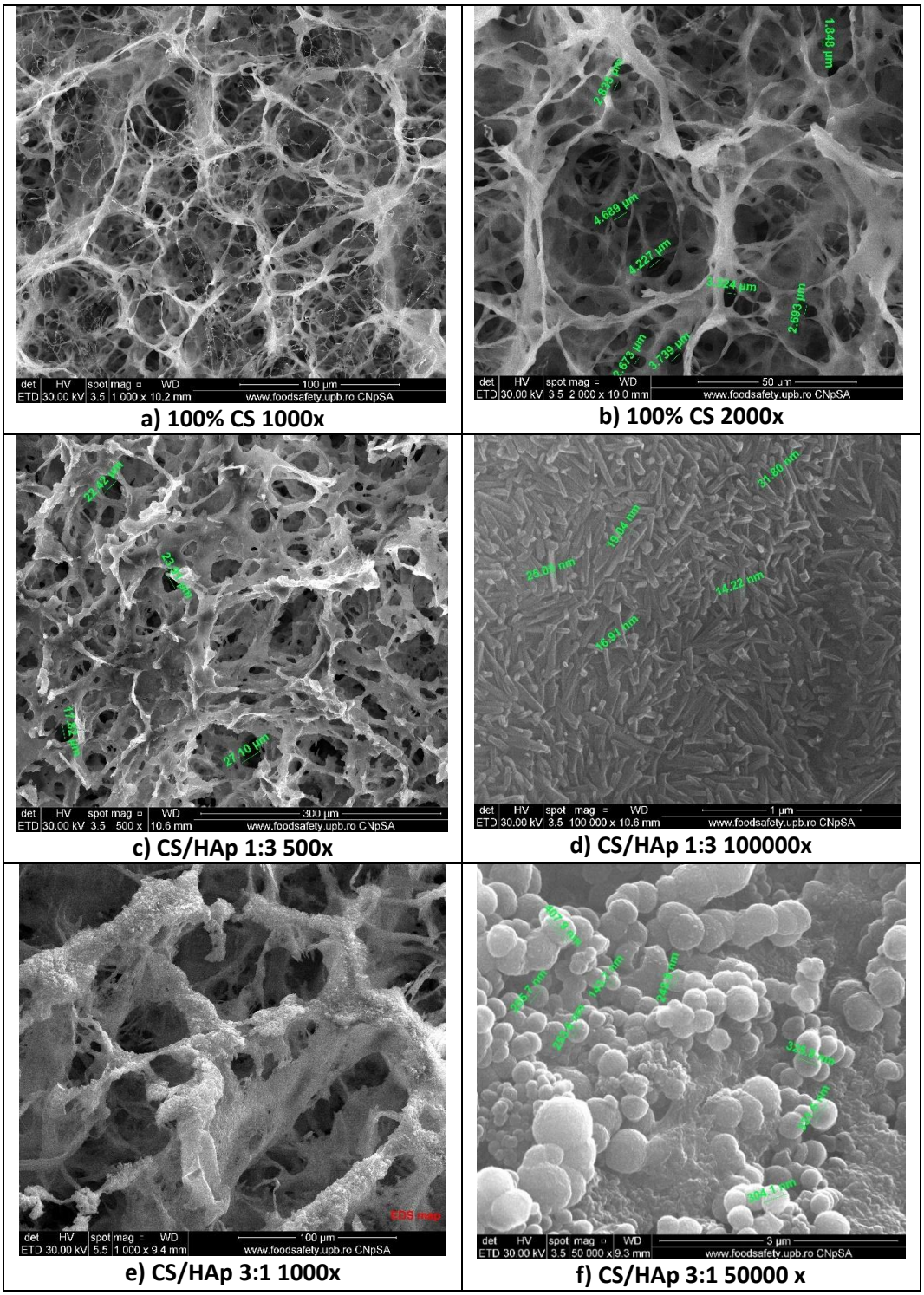

Fig 4. SEM images of chitosan and chitosan/hydroxyapatite structures

Fig. 4 shows the SEM images obtained for the chitosan (images a and b) and chitosan/hydroxyapatite scaffold (images c – f). From the analysis of these images, the fibrillar structure of chitosan matrix can be observed. It appears that freeze drying improves scaffold`s morphology. Scaffolds possess an open structure, with interconnected pores and good pores distribution. Figs. a) and b) show the fibrils connected by even thinner ones and a high porosity. Fig. 4 d) highlights the same fibrillar morphology, although the fibrils appear thicker due to the mineralization process. The interconnected pores have sizes between 17-27 μm. In Fig. 4 e) the inorganic phase composed of rod shape minerals can be observed. These rods have nanometric dimensions with width between 14.22-31.8 nm. Figs. 4 e) and 4 f) show a better mineralization of chitosan fibrils. This time they have a sphere-like shape with diameters between 100-465 nm. These spheres are made of even smaller ones.

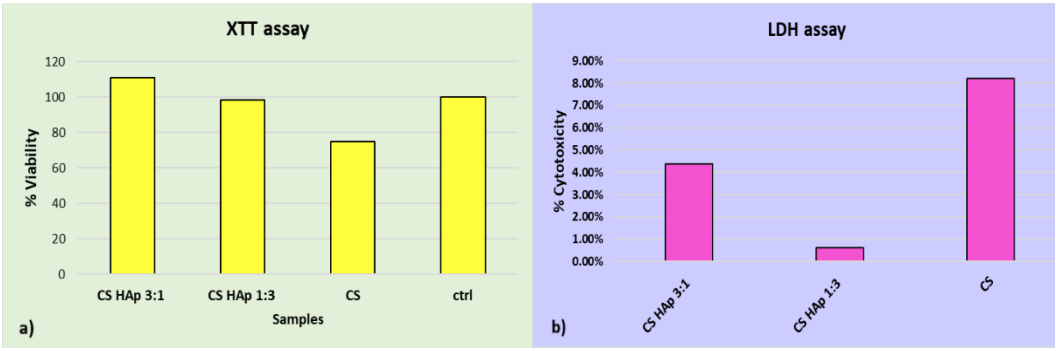

Fig.5. Viability of osteoblasts a) and cytotoxicity of composite systems b)

Fig. 5 a) shows the osteoblast`s viability evaluated by XTT assay for the three scaffolds. All samples have great biocompatibility, best results being registered for the composite systems, comparable to the control due to the presence of hydroxyapatite which is a well-known promoter of proliferation and osteogenesis. The results of the LDH assay, regarding the cytotoxic potential of the obtained scaffolds (Fig. 5 b) show no significant cytotoxic effect with values between 0.62-8.20%. The 100% chitosan scaffold has the highest level of cytotoxicity (8.20%), but it`s still far below the limit of concerns. Therefore, all composite materials have high biocompatibility making them suitable candidates for bone tissue repair and open new ways to develop drug delivery systems for BTE, from pure regeneration to the treatment of different diseases.

6. Conclusions

The study presents the synthesis of chitosan/hydroxyapatite (CS/HAp) based composite systems for BTE. The samples were obtained by freeze drying after the *in situ* generation of hydroxyapatite inside the chitosan matrix. The

characterization of the samples confirmed the formation of hydroxyapatite with different morphologies (spheres, rods) and nanometric dimensions. The composite systems showed great biocompatibility when tested on osteoblast cells and very low toxicity which makes them great candidates for bone tissue repair. These samples will be further loaded with a mixture of natural/synthetic active substances in order to be used in bone cancer treatment.

Acknowledgements:

The financial support within the RO-MD Project No. 29/20.05.2024 "Nanostructured bone grafts with predetermined properties" is highly acknowledged.

R E F E R E N C E S

1. Van der Stok, J., E.M.M. Van Lieshout, Y. El-Massoudi, G.H. Van Kralingen, and P. Patka, Bone substitutes in the Netherlands – A systematic literature review. Acta Biomaterialia, 2011. **7**(2): p. 739-750.
2. Sadeghzade, S., J. Liu, H. Wang, X. Li, J. Cao, H. Cao, B. Tang, and H. Yuan, Recent advances on bioactive baghdadite ceramic for bone tissue engineering applications: 20 years of research and innovation (a review). Materials Today Bio, 2022. **17**: p. 100473.
3. Otilia Ruxandra, V., S. Ioana, A. Ecaterina, T. Roxana, S. Vasile Adrian, O. Ovidiu, I. Andreia, and V. Bogdan Ştefan, Influence of the size and the morphology of ZnO nanoparticles on cell viability. Comptes Rendus. Chimie, 2015. **18**(12): p. 1335-1343.
4. Shao, X., Y. Wu, M. Ding, X. Chen, T. Zhou, C. Huang, X. Wang, C. Zong, Y. Liu, L. Tian, J. Qiao, Y. Liu, and Y. Zhao, Strong and tough β-TCP/PCL composite scaffolds with gradient structure for bone tissue engineering: Development and evaluation. Ceramics International, 2024. **50**(18, Part A): p. 31905-31917.
5. Alshemary, A.Z., S. Bilgin, G. Işık, A. Motameni, A. Tezcaner, and Z. Evis, Biomechanical Evaluation of an Injectable Alginate / Dicalcium Phosphate Cement Composites for Bone Tissue Engineering. Journal of the Mechanical Behavior of Biomedical Materials, 2021. **118**: p. 104439.
6. Mohagheghiyan, K., H. Mokhtari, and M. Kharaziha, Gelatin-coated mesoporous forsterite scaffold for bone tissue engineering. Ceramics International, 2024. **50**(8): p. 13526-13535.
7. Min, K.H., D.H. Kim, K.H. Kim, J.-H. Seo, and S.P. Pack Biomimetic Scaffolds of Calcium-Based Materials for Bone Regeneration. Biomimetics, 2024. **9**, DOI: 10.3390/biomimetics9090511.
8. Ressler, A. Chitosan-Based Biomaterials for Bone Tissue Engineering Applications: A Short Review. Polymers, 2022. **14**, DOI: 10.3390/polym14163430.
9. Mansouri, R., Y. Jouan, E. Hay, C. Blin-Wakkach, M. Frain, A. Ostertag, C. Le Henaff, C. Marty, V. Geoffroy, P.J. Marie, M. Cohen-Solal, and D. Modrowski, Osteoblastic heparan sulfate glycosaminoglycans control bone remodeling by regulating Wnt signaling and the crosstalk between bone surface and marrow cells. Cell Death & Disease, 2017. **8**(6): p. e2902-e2902.
10. Abu Elella, M.H. and O.M. Kolawole, Recent advances in modified chitosan-based drug delivery systems for transmucosal applications: A comprehensive review. International Journal of Biological Macromolecules, 2024. **277**: p. 134531.

11. Kim, I.-Y., S.-J. Seo, H.-S. Moon, M.-K. Yoo, I.-Y. Park, B.-C. Kim, and C.-S. Cho, Chitosan and its derivatives for tissue engineering applications. Biotechnology Advances, 2008. **26**(1): p. 1-21.
12. Venkatesan, J. and S.-K. Kim Chitosan Composites for Bone Tissue Engineering—An Overview. Marine Drugs, 2010. **8**, 2252-2266 DOI: 10.3390/md8082252.
13. Girón, J., E. Kerstner, T. Medeiros, L. Oliveira, G.M. Machado, C.F. Malfatti, and P. Pranke, Biomaterials for bone regeneration: an orthopedic and dentistry overview. Brazilian Journal of Medical and Biological Research, 2021. **54**.
14. Alkaron, W., A. Almansoori, K. Balázsi, and C. Balázsi Hydroxyapatite-Based Natural Biopolymer Composite for Tissue Regeneration. Materials, 2024. **17**, DOI: 10.3390/ma17164117.
15. Gomes, D.S., A.M.C. Santos, G.A. Neves, and R.R. Menezes, A brief review on hydroxyapatite production and use in biomedicine. Cerâmica, 2019. **65**.
16. Ma, R. and D. Guo, Evaluating the bioactivity of a hydroxyapatite-incorporated polyetheretherketone biocomposite. J Orthop Surg Res, 2019. **14**(1): p. 32.
17. Wong, S.K., M.M. Yee, K.-Y. Chin, and S. Ima-Nirwana A Review of the Application of Natural and Synthetic Scaffolds in Bone Regeneration. Journal of Functional Biomaterials, 2023. **14**, DOI: 10.3390/jfb14050286.
18. Abida, F., A. Elouahli, A. Bourouisse, M. Jamil, M. Gourri, Z. Ezzahmouly, and Hatim, Mechanism of Hydroxyapatite/Chitosan Composite Precipitation From Aqueous Solution at Room Temperature and Alkali Environment. 2016. **7**.
19. T. Szatkowski, A.K.-R., J. Zdarta, K. Szwarc-Rzepka, D. Paukszta, M. Wysokowski, H. Ehrlich, T. Jesionowski, Synthesis and characterization of hydroxyapatite/chitosan composites. Physicochem. Probl. Miner. Process., 2015. **51**(2): p. 575-585.
20. Hu, Y., J. Chen, T. Fan, Y. Zhang, Y. Zhao, X. Shi, and Q. Zhang, Biomimetic mineralized hierarchical hybrid scaffolds based on in situ synthesis of nano-hydroxyapatite/chitosan/chondroitin sulfate/hyaluronic acid for bone tissue engineering. Colloids and Surfaces B: Biointerfaces, 2017. **157**: p. 93-100.
21. Shi, D., J. Shen, Z. Zhang, C. Shi, M. Chen, Y. Gu, and Y. Liu, Preparation and properties of dopamine-modified alginate/chitosan–hydroxyapatite scaffolds with gradient structure for bone tissue engineering. Journal of Biomedical Materials Research Part A, 2019. **107**(8): p. 1615-1627.
22. Du, X., T. Wang, and S. Chen, Synthesis and in vitro biodegradability of carbonatedhydroxyapatite/chitosan composite spheres. IOP Conference Series: Materials Science and Engineering, 2018. **382**(2): p. 022007.
23. Bushra, A., A. Subhani, and N. Islam, A comprehensive review on biological and environmental applications of chitosan-hydroxyapatite biocomposites. Composites Part C: Open Access, 2023. **12**: p. 100402.
24. Wang, H., R. Sun, S. Huang, H. Wu, and D. Zhang, Fabrication and properties of hydroxyapatite/chitosan composite scaffolds loaded with periostin for bone regeneration. Heliyon, 2024. **10**(5): p. e25832.
25. Motelica, L., D. Ficai, A. Ficai, R.-D. Trușcă, C.-I. Ilie, O.-C. Oprea, and E. Andronescu Innovative Antimicrobial Chitosan/ZnO/Ag NPs/Citronella Essential Oil Nanocomposite—Potential Coating for Grapes. Foods, 2020. **9**, DOI: 10.3390/foods9121801.